Supplementary Information (SI) for New Journal of Chemistry.

Illuminating Multi-Stage Sodium Storage in High-Rate Porous Hard Carbon: Mechanistic Insights from Pore Architecture

Yulin MAO, Yueyang WANG, Yuyang ZHAO, Qingyuan LI, Guoxing SUN and Guichuan XING**

Y. L. Mao, Y. Y. Wang, Y. Y. Zhao, Q. Y. Li, Prof. G. X. Sun and Prof. G. C. Xing

Institute of Applied Physics and Materials Engineering, University of Macau, Avenida da Universidade, Taipa, Macau SAR, China.

Email: gxsun@um.edu.mo, gcxing@um.edu.mo

Experimental section

Materials Synthesis

Zinc gluconate (purity: 98%, purchased from MACKLIN) and glucose (purity: >99.5%, purchased from MACKLIN) were used as precursors for the synthesis of porous hard carbon. The synthesis process for HC-1, HC-2, and HC-3 is depicted schematically in Figure 1.

For the preparation of HC-1, zinc gluconate and glucose were mixed at a molar ratio of 1:1 and dissolved in deionized water to form a precursor solution. The solution was gradually frozen in a refrigerator to reduce the cooling rate. The frozen samples were then freeze-dried by transferring the powder into a 200 mL beaker and drying them in a freeze dryer for 12 hours. The resulting freeze-dried samples were pyrolyzed in a tube furnace under an argon atmosphere. During pyrolysis, argon gas was continuously flowed into the furnace, and the temperature was ramped to 1300°C at a rate of 15°C/min, maintained at 1300°C for 2 hours, and then naturally cooled to room temperature.

For HC-2, the precursor solution was prepared in the same way as HC-1. However, instead of gradual freezing, the precursor solution was added in small portions into an excess of liquid nitrogen to achieve rapid and uniform quenching of zinc gluconate crystals at the nanoscale. This flash-freezing process facilitated the formation of nanoscale zinc gluconate crystals, which, upon pyrolysis, generated nanoscale ZnO. The nanoscale ZnO acted as an etching agent for the carbon matrix, significantly increasing the micropore content of HC-2 and enhancing its sodium storage performance. After flash freezing, the samples were freeze-dried under the same conditions as HC-1 and then pyrolyzed using the same procedure.

To better visualize the morphology of zinc oxide nanoparticles in HC-2 and the pore structure introduced by these nanoparticles into the HC-2 sample, the freeze-dried precursor was heated in a tubular furnace under argon atmosphere protection. The temperature was raised to 700°C at a heating rate of 10°C/min, maintained for 1 hour, and then allowed to cool naturally. The resulting sample was designated as HC-2-ZnO.

For HC-3, zinc gluconate and glucose powders were directly mixed at a molar ratio of 1:1 via mechanical grinding. The ground mixture was pyrolyzed without undergoing any freezing or freeze-drying steps, following the same pyrolysis conditions as HC-1 and HC-2.

Materials Characterizations

The morphology of the HC samples was analyzed using a Scanning Electron Microscope (SEM, Zeiss Sigma FESEM). The crystalline structure was examined by X-ray diffraction (XRD) using a Rigaku SmartLab 9 kW diffractometer equipped with Cu Kα radiation ($\lambda = 0.15418$ nm) under operating conditions of 40 kV and 200 mA. Raman spectroscopy (Thermo Fisher Scientific DXR3) with a 532 nm laser was employed to qualitatively analyze molecular vibrations and rotational transitions in the carbon framework. To evaluate the specific surface area and pore size distribution, nitrogen adsorption-desorption isotherms were measured at 77.490 K using a Micromeritics 3 Flex 5.00 system. For electrode composition analysis, X-ray photoelectron spectroscopy (XPS, ESCALAB 250i) was conducted under Ar protection. Depth profiling was performed using an argon ion gun (beam energy: 2000 eV) with etching depth of 0, 2.5, 5, 10, and 20 nm.

Electrochemical Measurements

Electrochemical tests were carried out using HC powders as anodes. To prepare the electrodes, a slurry was made by mixing the active material, PVDF binder, and Ketjenblack EC600JD in a mass ratio of 8:1:1. The slurry was uniformly coated onto a copper foil substrate to achieve a thickness of approximately 20 μm. The coated electrodes were then dried at 80°C in a vacuum oven for 12 hours before being punched into 12 mm circular disks. CR2025 coin cells were fabricated in an argon-filled glove box, utilizing 160 μL of 1 mol L^{-1} $NaPF_6$ dissolved in diglyme as the electrolyte, a Whatman GF/D glass-fiber separator, and a 16 mm sodium sheet on an aluminum current collector. Galvanostatic charge-discharge (GCD) and galvanostatic intermittent titration technique (GITT) tests were conducted using a NEWARE BTS4000 system at 30°C within a voltage range of 0.01–2.5 V. The sodium ion diffusion coefficient (D_{Na^+}) was calculated based on a simplified form of Fick's second law as follows:

$$D^{GITT} = \frac{4}{\Pi\tau}\left(\frac{m_B V_m}{M_B S}\right)^2\left(\frac{\Delta E_S}{\Delta E_t}\right)^2$$

Where τ is the pulse duration (s), mB is the active mass of the HCM electrode (g), MB is the molar mass of hard carbon (g mol^{-1}), Vm is the molar volume (cm^3 mol^{-1}), and S is the active surface area of the electrode (m^2 g^{-1}). The parameters ΔEs (measured after 10 min) and ΔEτ (measured after 180 min) were extracted from GITT curves. Cyclic voltammetry (CV) was performed at a scan rate of 0.1-1 mV s^{-1}, and electrochemical impedance spectroscopy (EIS) was measured using a CHI660E electrochemical workstation. To investigate sodium storage behavior, the 5th cycle GCD curves were recorded at a current density of 20 mA g^{-1} within a voltage window of 0.01–2.5 V versus Na^+/Na.

Ex-situ Characterizations

Ex-situ Raman spectroscopy was performed using a customized electrolytic cell equipped with a quartz observation window. During the test, the cells were discharged to specific voltage values at a current density of 40 mA g^{-1}. For ex-situ characterization, including XPS, TEM, and SAXS, the electrodes were harvested from cycled cells disassembled inside an argon-filled glove box. The electrodes were thoroughly rinsed with diglyme to remove residual electrolyte and impurities. Subsequently, the cleaned samples were transferred to the testing chamber using a sealed sample transfer device to prevent exposure to the ambient atmosphere.

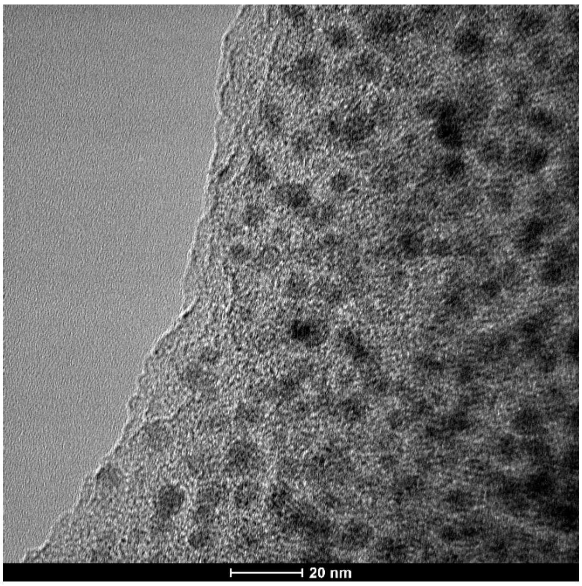

Figure S1 TEM image of HC-2-ZnO.

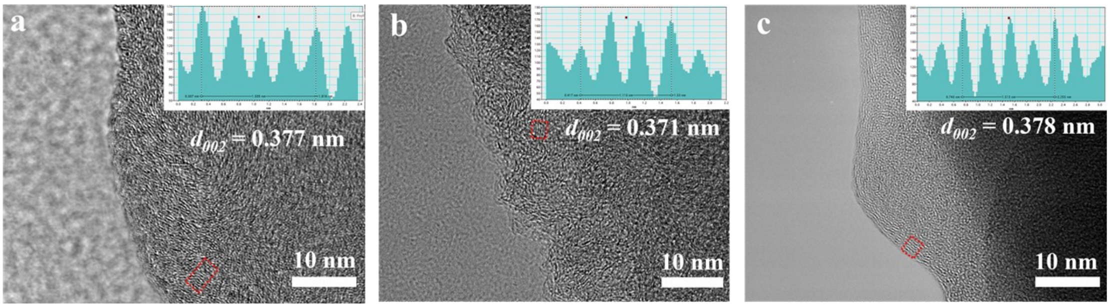

Figure S2 d_{002} measurement of HC-1, HC-2 and HC-3.

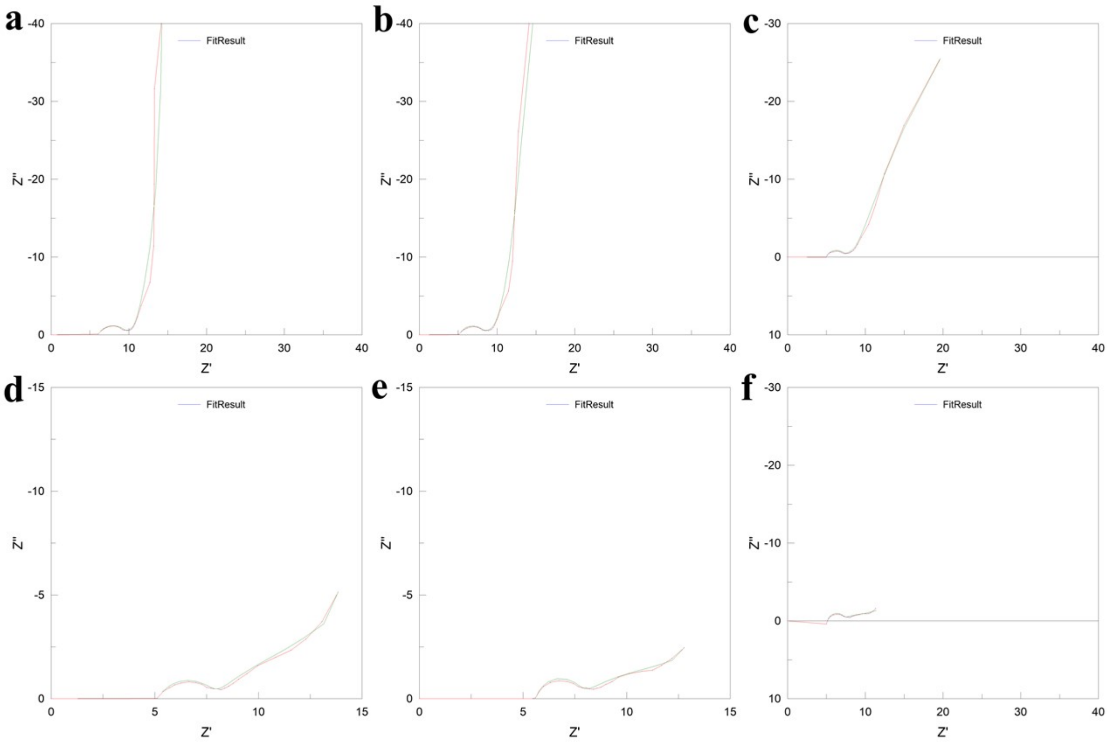

Figure S3 Nyquist plots and the fitted curves of HC-2 at 2.5 V, 0.9 V, 0.6 V, 0.1 V, 0.05 V, 0.01 V, respectively.

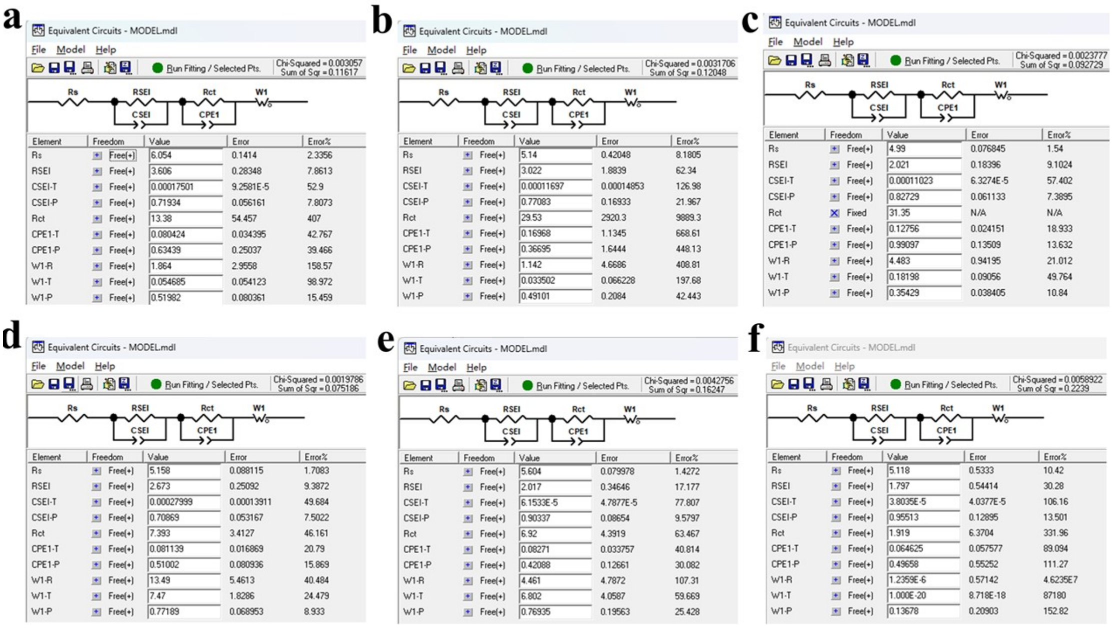

a

Chi-Squared = 0.003057
Sum of Sqr = 0.11617

Element	Freedom	Value	Error	Error%
Rs	Free(+)	6.054	0.1414	2.3356
RSEI	Free(+)	3.606	0.28348	7.8613
CSEI-T	Free(+)	0.00017501	9.2581E-5	52.9
CSEI-P	Free(+)	0.71934	0.056161	7.8073
Rct	Free(+)	13.38	54.457	407
CPE1-T	Free(+)	0.080424	0.034395	42.767
CPE1-P	Free(+)	0.63439	0.25037	39.466
W1-R	Free(+)	1.864	2.9558	158.57
W1-T	Free(+)	0.054685	0.054123	98.972
W1-P	Free(+)	0.51982	0.080361	15.459

b

Chi-Squared = 0.0031706
Sum of Sqr = 0.12048

Element	Freedom	Value	Error	Error%
Rs	Free(+)	5.14	0.42048	8.1805
RSEI	Free(+)	3.022	1.8839	62.34
CSEI-T	Free(+)	0.00011697	0.00014853	126.98
CSEI-P	Free(+)	0.77083	0.16933	21.967
Rct	Free(+)	29.53	2920.3	9889.3
CPE1-T	Free(+)	0.16968	1.1345	668.61
CPE1-P	Free(+)	0.36695	1.6444	448.13
W1-R	Free(+)	1.142	4.6686	408.81
W1-T	Free(+)	0.033502	0.066228	197.68
W1-P	Free(+)	0.49101	0.2084	42.443

c

Chi-Squared = 0.0023777
Sum of Sqr = 0.092729

Element	Freedom	Value	Error	Error%
Rs	Free(+)	4.99	0.076845	1.54
RSEI	Free(+)	2.021	0.18396	9.1024
CSEI-T	Free(+)	0.00011023	6.3274E-5	57.402
CSEI-P	Free(+)	0.82729	0.061133	7.3895
Rct	☒ Fixed	31.35	N/A	N/A
CPE1-T	Free(+)	0.12756	0.024151	18.933
CPE1-P	Free(+)	0.99097	0.13509	13.632
W1-R	Free(+)	4.483	0.94195	21.012
W1-T	Free(+)	0.18198	0.09056	49.764
W1-P	Free(+)	0.35429	0.038405	10.84

d

Chi-Squared = 0.0019786
Sum of Sqr = 0.075186

Element	Freedom	Value	Error	Error%
Rs	Free(+)	5.158	0.088115	1.7083
RSEI	Free(+)	2.673	0.25092	9.3872
CSEI-T	Free(+)	0.00027999	0.00013911	49.684
CSEI-P	Free(+)	0.70869	0.053167	7.5022
Rct	Free(+)	7.393	3.4127	46.161
CPE1-T	Free(+)	0.081139	0.016869	20.79
CPE1-P	Free(+)	0.51002	0.080936	15.869
W1-R	Free(+)	13.49	5.4613	40.484
W1-T	Free(+)	7.47	1.8286	24.479
W1-P	Free(+)	0.77189	0.068953	8.933

e

Chi-Squared = 0.0042756
Sum of Sqr = 0.16247

Element	Freedom	Value	Error	Error%
Rs	Free(+)	5.604	0.079978	1.4272
RSEI	Free(+)	2.017	0.34646	17.177
CSEI-T	Free(+)	6.1533E-5	4.7877E-5	77.807
CSEI-P	Free(+)	0.90337	0.08654	9.5797
Rct	Free(+)	6.92	4.3919	63.467
CPE1-T	Free(+)	0.08271	0.033757	40.814
CPE1-P	Free(+)	0.42088	0.12661	30.082
W1-R	Free(+)	4.461	4.7872	107.31
W1-T	Free(+)	6.802	4.0587	59.669
W1-P	Free(+)	0.76935	0.19563	25.428

f

Chi-Squared = 0.0058922
Sum of Sqr = 0.2239

Element	Freedom	Value	Error	Error%
Rs	Free(+)	5.118	0.5333	10.42
RSEI	Free(+)	1.797	0.54414	30.28
CSEI-T	Free(+)	3.8035E-5	4.0377E-5	106.16
CSEI-P	Free(+)	0.95513	0.12895	13.501
Rct	Free(+)	1.919	6.3704	331.96
CPE1-T	Free(+)	0.064625	0.057577	89.094
CPE1-P	Free(+)	0.49658	0.55252	111.27
W1-R	Free(+)	1.2359E-6	0.57142	4.6235E7
W1-T	Free(+)	1.000E-20	8.718E-18	87180
W1-P	Free(+)	0.13678	0.20903	152.82

Figure S4 The fitted data of HC-2 at 2.5 V, 0.9 V, 0.6 V, 0.1 V, 0.05 V, 0.01 V, respectively.